6. Nonlinear vibrations: bifurcation analysis

The nonlinear response of the rotational-translational bulk model of planetary gear set is now analyzed in detail by means of bifurcation diagrams, Poincaré maps, phase portraits, time responses and spectra. The complex dynamics is analyzed via direct simulation. In order to obtain the Poincaré maps, time histories are sampled with the same frequency of the excitation. Poincaré sections are useful tools for analyzing chaotic responses. Moreover, bifurcation diagrams of the Poincaré maps can be drawn by varying one of the parameters, which govern the response of the system (the meshing frequency here). The equations of motion are integrated for a sufficiently long time in order to eliminate the transitory motion, then a certain number of periods are considered. This procedure is repeated for different values of the parameter, using the final state of the system in the previous analysis as initial condition. The procedure allows a particular, stable solution to be followed when a parameter is varied regularly.

Numerical parameters of Tables 2, 3 and 5 are considered. Two different translational stiffnesses of planet bearings are investigated: K_p=2.19×10^{9}N/m (from Ref. [2]) and K_p=2.19×10^{8}N/m. Natural frequencies of each case are listed in Table 8.

Table 8: Comparison of Natural frequencies for rotational-translational model

Frequency mode number	Natural frequency [Hz] case 1: K_p=2.19×10^{9}N/m, Ref[2]	Natural frequency [Hz] case 2: K_p=2.19×10^{8}N/m
1	1758	959
2	1758	1445
3	2100	1445
4	3352	1921
5	3352	2035
6	5253	2035
7	6384	3574
8	6384	3574
9	7190	5166
10	7405	5166
11	7405	5209
12	8542	7067
13	8572	7473
14	8572	7473
15	22378	22376
16	22378	22376
17	53264	53207
18	149115	149115

The comparison between two cases in Table 8 shows that stiffness of the planet bearings has bigger influence on low natural frequencies. The higher natural frequencies are similar in both cases, while the fundamental frequency of the first case is more than two times the one of the second case. The *symmetry* of the system gives rise to double modes.

The main excitation frequency of the system is the meshing frequency of the planetary gear. The amplitude of external excitation is related to the external torque on the sun gear. Behind the main excitation, there exist *internal resonances* due to the integer ratios between the natural frequencies of the system. We show the change of nonlinear phenomena between the systems with and without internal resonances.

For the two cases the internal resonances are summarized below:

Case 1 of Table 8: $\omega_7 \cong 2\times\omega_4$, $\omega_{15} \cong 6\times\omega_6$

Case 2 of Table 8: $\omega_4 \cong 2\times\omega_1$, $\omega_9 \cong 2\times\omega_5$

In the case 2, the internal resonances involve the fundamental frequency, so that the resulting vibration is more significant.

The bifurcation diagrams are extracted by varying the mesh frequency; 750 frequencies (upward) are analyzed, for each one the integration is carried out for 1000 periods, the last 50 periods are recorded and the initial 950 periods are disregarded in order to remove the transient vibrations; when the frequency is changed the new simulation is carried out using the final state of the previous simulation as initial condition with a small perturbation; the sampling frequency is equal to the excitation frequency in order to build the Poincaré maps. Figs. 7 and 8 show bifurcation diagrams vs. excitation mesh frequency for the case 1 and 2, respectively. Figs. 7(a) and 8(a) represent the bifurcation diagrams of sun rotation and Figs. 7(b) and 8(b) represent the bifurcation diagram of first planet rotation. Damping properties used for these two models are listed in the first row (low frequency range) of Table 3.

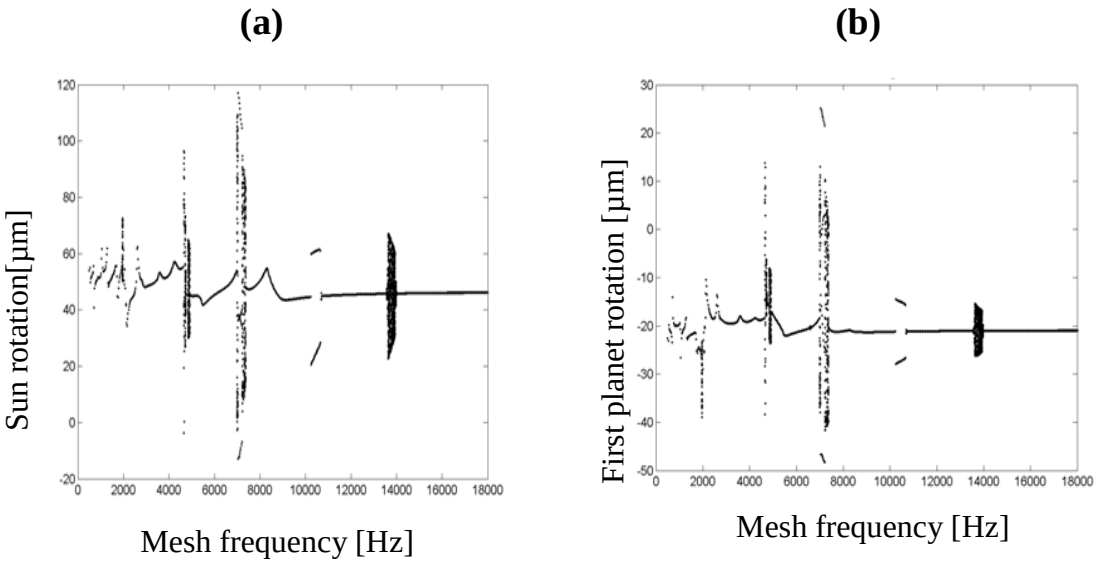

Fig. 7. Bifurcation diagram vs. mesh frequency for case 1: (a) sun rotation (b) first planet rotation

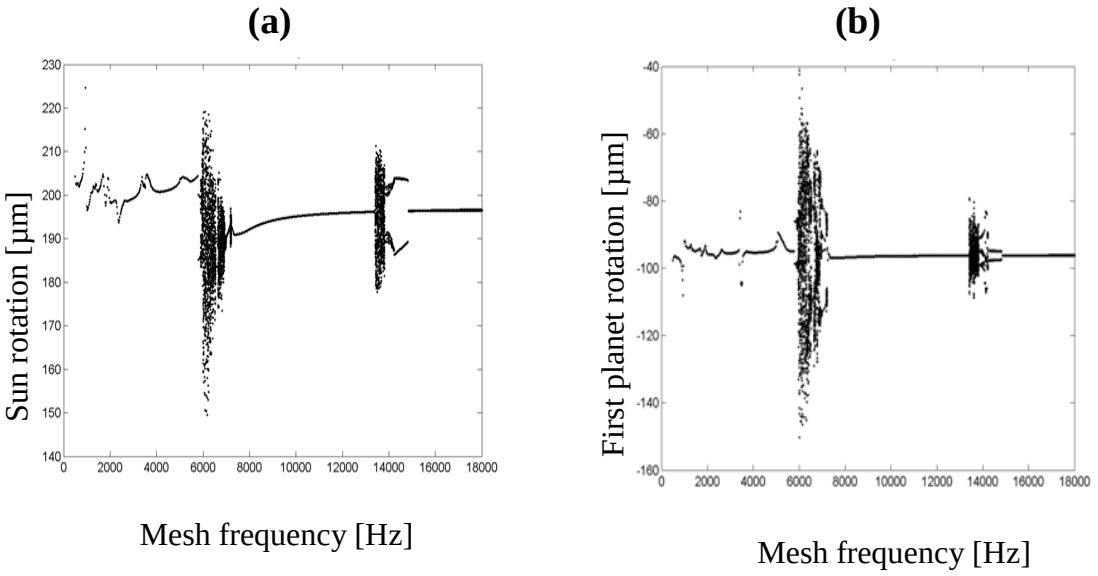

Fig. 8. Bifurcation diagram vs. mesh frequency for case 2 (a) sun rotation (b) first planet rotation

In Figs. 7 and 8 periodic responses can be identified by a single line. For both cases, the responses for the mesh frequencies higher than 15000 Hz are periodic, this is reasonable because there are no frequencies between (8572-22378) Hz for case 1 and (7473-22376) Hz for case 2. From Fig. 7 (for case 1) it can be observed that the bifurcation diagram crosses a 2T region at $\omega_m \in$(10200-10700) Hz, where the period of response is twice the excitation period; this 2T region disappears for case 2. The route from 1T to 2T regimes is discontinuous, i.e. there is a jump, this is due to the presence of

piecewise linear spring combined with time varying stiffness, it is typical of gear dynamics; this appears both for sun rotation, Fig. 7(a), and first planet rotation, Fig. 7(b).

In the mesh frequency range $\omega_m \in$(5750-7000) Hz, case 2, Fig. 8 indicates the onset of gear tooth separation and chaotic response; because $\omega_4=2\times\omega_1$, the third harmonic of ω_4 and the 6th harmonic of ω_1, overlap with 4th harmonic of $\omega_{2,3}$=1445 Hz, this is probably the reason of the chaotic region. Inside the interval $\omega_m \in$(7000-7200) Hz, close to a rotational mode resonance, a 2T region takes place for 1st planet rotation although the motion is chaotic for sun rotation, see Fig. 8 and Table 9. Another chaotic region appears at $\omega_m=\omega_{12}$=7182 Hz. A sudden disappearance of a chaotic orbit is often called blue-sky catastrophe; however, another motivation for a sudden change of dynamics can be the presence of coexisting stable chaotic and regular orbits, Ref. [37].

At frequency range $\omega_m \in$(13400-13800) Hz, Fig. 6, there is another chaotic region which leads to 4T region at the frequency range $\omega_m \in$(13800-14200) Hz. A further 2T region, appears for $\omega_m \in$(14200-14800) Hz.

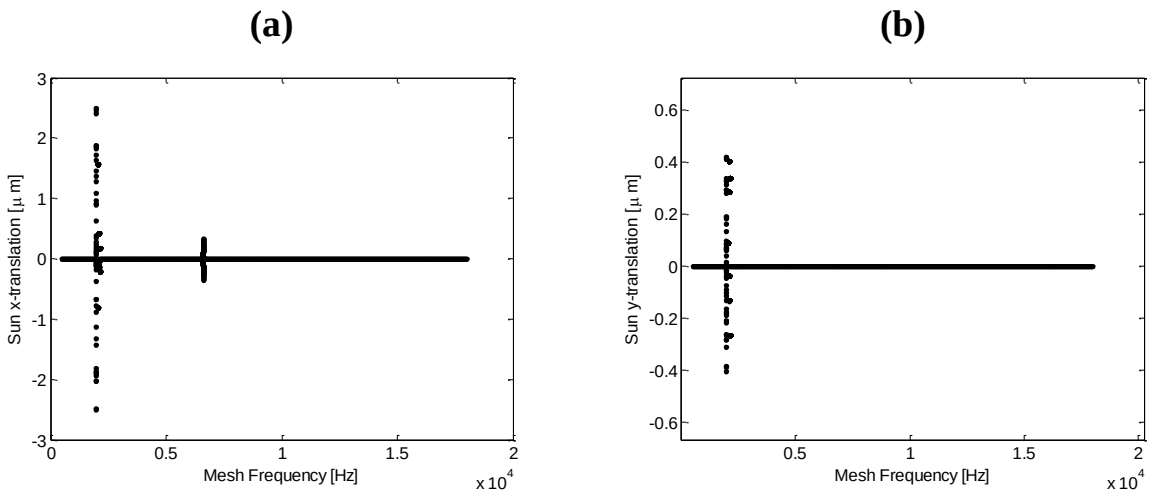

Fig. 9. Bifurcation diagram vs. mesh frequency for case 1 (a)Sun center *x*-translation [μm](b) Sun center *y*-translation [μm]

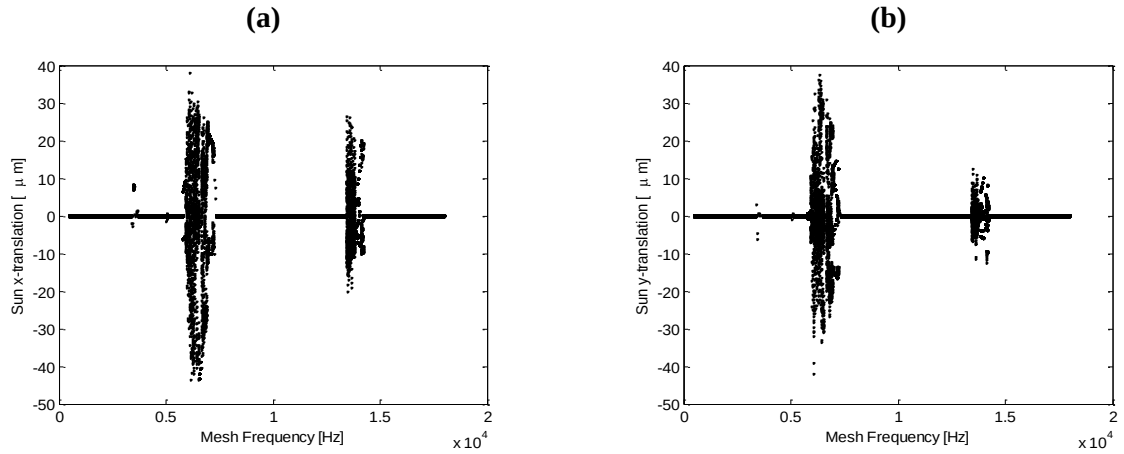

Fig. 10. Bifurcation diagram vs. mesh frequency for case 2 (a)Sun center *x*-translation [μm](b) Sun center *y*-translation [μm]

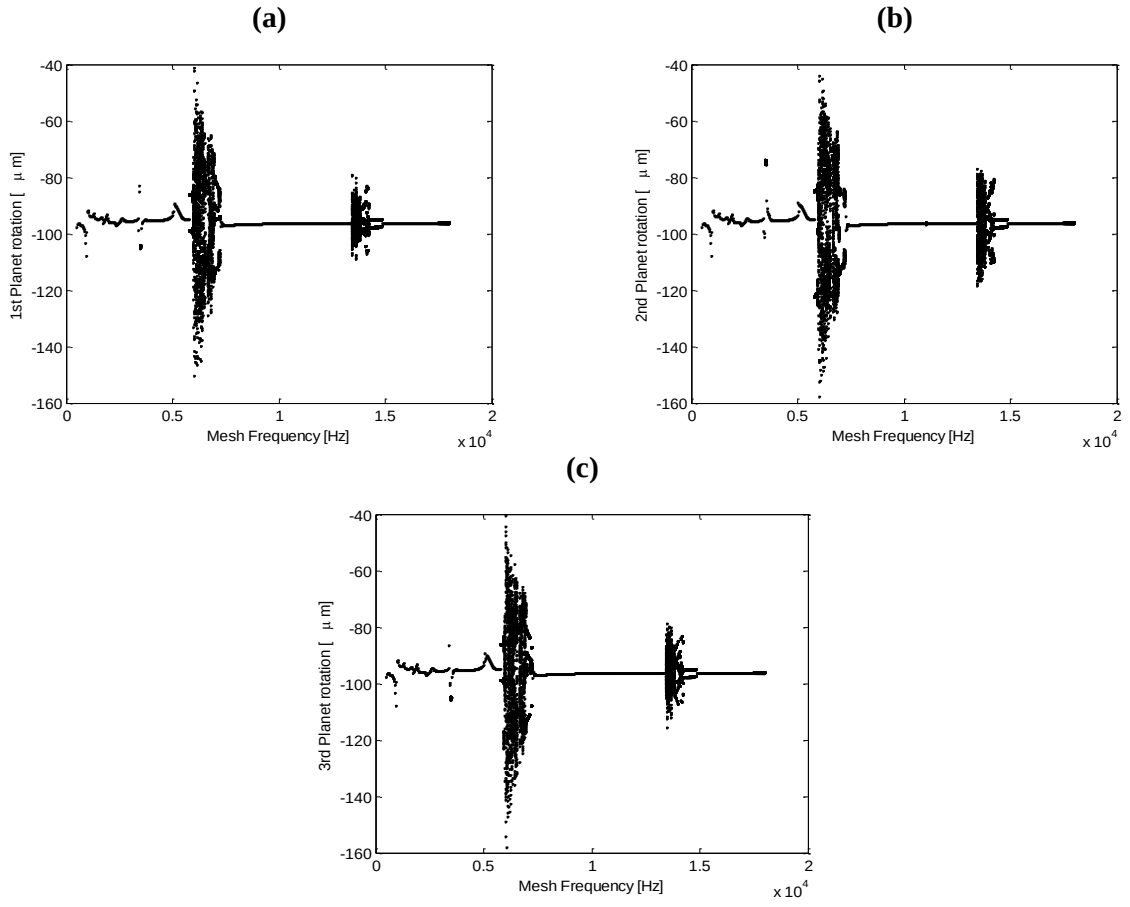

Fig. 11. Bifurcation diagram vs. mesh frequency for case 2 (a)first planet rotation[μm],(b) second planet rotation [μm], (c)third planet rotation [μm].

Figs. 9 and 10 give additional and extremely important information about the system dynamics for the case 2. Fig. 10(a) corresponds to *x*-translation of sun gear center and Fig. 10(b) corresponds to its *y*-translation. In linear field, the symmetry and the perfect balancing of the system implies that the sun is loaded with a self-equilibrate force system from the planets, therefore it should experience no displacement in *x* and *y* directions. This is particularly evident in the case 2 Fig. 10. For the ranges where complex phenomena appear, the system presents symmetry breaking and consequently sun imbalance. Fig. 11 presents the bifurcation diagram for all planets rotations. All planets undergo to the same vibration except for the chaotic regions when the symmetry breaking is evident.

Now the most interesting regimes found in the bifurcation diagrams are analyzed in detail. For each regime Poincaré maps, phase portraits, spectra and time histories are shown, see Table 9.